

Surface morphology and kinetic roughening of Ag on Ag(111) studied with scanning tunneling microscopy

I. Heyvaert,* J. Krim,† C. Van Haesendonck, and Y. Bruynseraede

Laboratorium voor Vaste-Stoffysica en Magnetisme, Katholieke Universiteit Leuven, Celestijnenlaan 200 D, B-3001 Heverlee, Belgium

(Received 4 January 1996)

The topography of Ag grown on Ag(111) measured with scanning tunneling microscopy reveals three-dimensional, layered islands for film thicknesses below 500 Å. For thicker Ag films, the layered structures can no longer be observed. The induced surface roughness increases with increasing film thickness and corresponds to the formation of self-similar surfaces with roughness exponents H close to 1 for thicknesses up to 5000 Å. Our results are compared to the relevant theoretical models. [S1063-651X(96)11307-6]

PACS number(s): 05.40.+j, 61.16.Ch, 68.35.Bs, 68.55.-a

I. INTRODUCTION

In deposition processes used to fabricate thin solid films, one observes a very strong dependence of the film microstructure and the surface roughness on the growth conditions. A study of this microstructure and of the surface roughness might help to reveal the underlying growth mechanisms. This is important since the film structure as well as the surface roughness have a profound influence on the physical properties of the film.

The growth of vapor-deposited films has been extensively studied. Growth models have been developed that take into account different physical processes. Films deposited under nonequilibrium conditions have recently also been the subject of many atomic-scale computer simulations and applications of the scaling theory [1–5]. In many cases, interfaces growing under nonequilibrium conditions (which is the case for most thin-film deposition processes) evolve into self-affine surfaces [1,6–14]. In this case, the root-mean-square (RMS) roughness σ increases with the size L of the surface as $\sigma(L) \propto L^H$, where the scaling exponent H ($0 \leq H \leq 1$), called the roughness exponent, is indicative of the topography of the surface. This regime of self-affine scaling is valid for length scales smaller than the correlation length ξ . At length scales exceeding the correlation length, the roughness reaches a saturation value σ_r . In dynamic processes, the roughness also changes as a function of the growth time [8–15]. Often, the saturated roughness σ_r increases in time as $\sigma_r \propto t^\beta$, until a certain maximum roughness value is reached. β , which is called the dynamic scaling exponent, is related to the temporal evolution of the roughness. The temporal and spatial behavior of the roughness can then be described by the dynamic scaling relation [18]:

$$\sigma(L, t) = L^H f(tL^{-H/\beta}),$$

*Permanent address: Laboratorium voor Chemische en Biologische Dynamica, Katholieke Universiteit Leuven, Celestijnenlaan 200 D, B-3001 Heverlee, Belgium.

†Permanent address: Department of Physics, Northeastern University, Huntington Avenue, Dana Bldg, Boston, MA 02115.

where f is a scaling function. For many growth models the characteristic scaling exponents have been calculated.

We have used the scanning tunneling microscope (STM) to study the topography and the evolution of the surface roughness during the growth of Ag on Ag(111). With the invention of various scanning probe microscopes, techniques became available to measure the surface roughness directly down to the nanometer scale. The surface roughness and the scaling exponents will be compared to exponents obtained from growth models in order to reveal the underlying growth mechanism.

II. EXPERIMENTAL PROCEDURE

Our STM (WA Technology Ltd., Cambridge) is installed in an ultrahigh vacuum (UHV) chamber (10^{-10} mbar) to which a deposition chamber is attached (10^{-7} mbar during the evaporation). In between the thermal evaporation of the different Ag layers, the sample can be transferred to the STM chamber without exposing the surface to air.

It is well known that the thermal evaporation of Ag on top of freshly cleaved mica at a temperature of 275 °C produces flat Ag(111) surfaces [16]. The mica substrate is introduced into the evaporation chamber in the vacuum system immediately after cleaving. Before evaporation of Ag, the mica is annealed at a temperature of 400 °C. The heating of the mica is obtained with an electron beam directed into a hole in the substrate holder towards the back side of the substrate. In order to obtain a uniform heating of the substrate, a silicon wafer is placed directly under the mica substrate. The substrate temperature is calibrated with a thermocouple attached to the front side of the mica substrate during a test evaporation. After deposition of the Ag(111) layer, the sample is cooled down to room temperature and transferred to the UHV chamber, where the surface topography and roughness are studied with STM.

On the Ag(111) surface at room temperature, gradually more and more Ag is evaporated. In between the evaporation of the different Ag layers, the sample is transferred to the STM chamber. The morphology as well as the RMS roughness as a function of the length scale have been determined for the various layer thicknesses. The procedure, which was followed to determine the roughness exponent, has been described elsewhere [17]. Briefly, a variety of scans (5–10

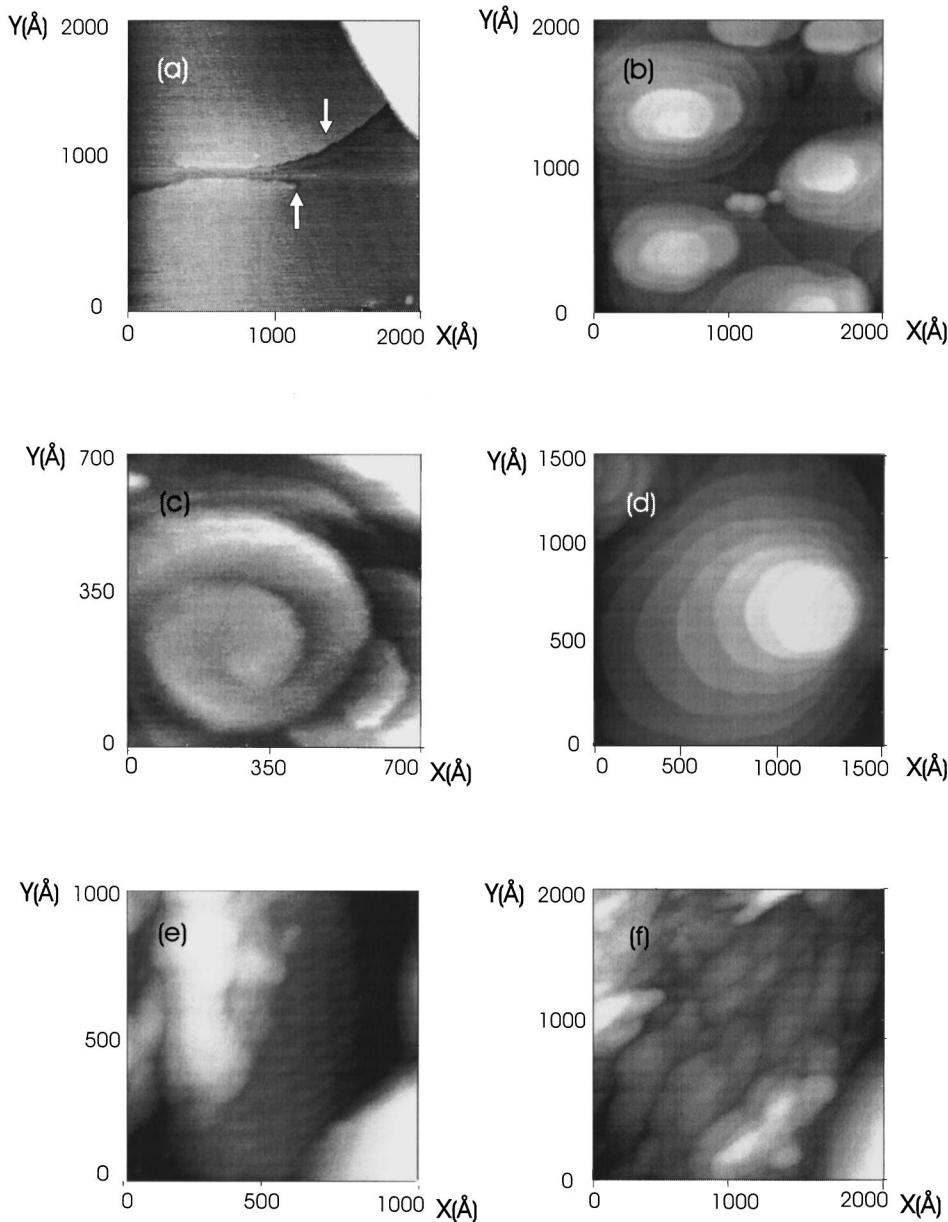


FIG. 1. STM pictures showing the Ag surface topography at various stages of the growth process. (a) Ag grown on mica at a temperature of 275 °C reveals large Ag(111) grains with atomically flat surfaces. On the grain surfaces atomic steps (see upper arrow) and growing defects (see lower arrow) can be found. The evolution of the topography of the Ag film evaporated at room temperature on top of the flat Ag(111) area is given for an average layer thickness of (b) 31 Å, (c) 31 Å, (d) 62 Å, (e) 483 Å, and (f) 1997 Å. In (c) a screw dislocation appearing on top of a Ag island grown on the Ag(111) surface is shown. The vertical scales (black to white) are (a) 22 Å, (b) 30 Å, (c) 25 Å, (d) 29 Å, (e) 40 Å, and (f) 141 Å.

typically), each of size L , are recorded at random locations on the surface. The RMS roughness values, given by the instrument software for the individual scans, are then averaged. As soon as the average roughness at that length scale does not change by more than 10%, when more images are averaged, data recording is stopped. This procedure is repeated for numerous different scan sizes, generating a set of average σ values as a function of the length scale L . The obtained data are then plotted in a $\log_{10}(\sigma)$ versus $\log_{10}(L)$ graph and a least-square fit to the data points is performed. The slope of the fitted curve determines the roughness exponent H .

III. EXPERIMENTAL RESULTS

The STM measurements on the original Ag(111) surface [shown in Fig. 1(a)] indicate that the maximum size of the atomically flat islands is about 2000 Å. The islands are separated by deep valleys. On top of the islands atomic steps as

well as dislocations can be observed [see arrows in Fig. 1(a)].

After evaporation of Ag on the Ag(111) surface at room temperature, circular, three-dimensional (3D) islands are growing on top of the atomically flat Ag(111) terraces. In Fig. 1(b) a typical image of the surface is shown after evaporation of 31 Å of Ag. The island size at the base line is 500–1000 Å. The steps between the terraces are one unit cell in height and the top layers become increasingly smaller, leading to a pyramidal-like structure. On some of these 3D islands, a screw dislocation can be observed [Fig. 1(c)]. When evaporating more and more Ag, the islands are growing higher. In Fig. 1(d), an island with a diameter of 1500 Å, which is comparable to the size of the underlying Ag(111) grain, is shown. The evaporated Ag thickness is 62 Å. A similar behavior is observed up to a Ag thickness of about 250 Å. At a thickness of around 500 Å, the surface topography has changed: the surface becomes more irregular and cloudy. Sometimes, in between this cloudy areas, the under-

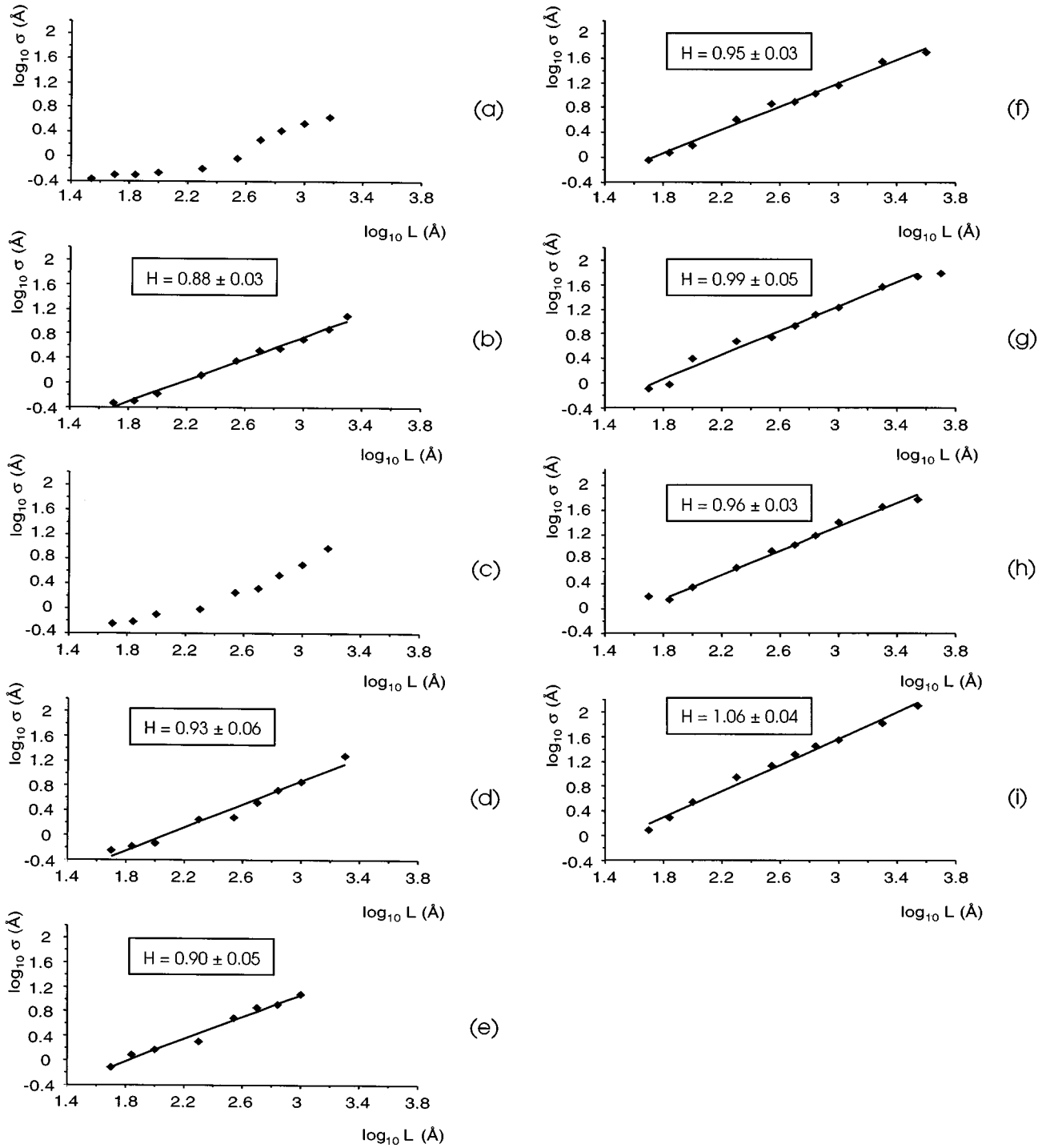


FIG. 2. $\log_{10}(\sigma)$ vs $\log_{10}(L)$ plot for the growth of the Ag film shown in Fig. 1, with L the scan size and σ the average RMS roughness: for (a) the Ag(111) substrate and for Ag layers with an average thickness of (b) 31 Å, (c) 62 Å, (d) 123 Å, (e) 243 Å, (f) 483 Å, (g) 963 Å, (h) 1997 Å, and (i) 5001 Å. The values of the roughness exponents H , indicated in each plot, are determined via a least-square fit restricted to the linear regime.

lying islands with atomic steps can still be observed [Fig. 1(e)]. In Fig. 1(f), the topography of a layer with a thickness of about 2000 Å is presented: the underlying topography is completely mimicked.

In Fig. 2, \log_{10} - \log_{10} plots of the RMS roughness σ as a function of the length scale L are shown for the different Ag layer thicknesses. The roughness increases with increasing length scale, but it is clear that the saturation value σ_t could

not be reached because of the limited scan range of our STM. Consequently, the dynamic scaling exponent β cannot be determined. On the other hand, we observe that the roughness values increase with increasing layer thickness. This increase is not very pronounced for the smaller thicknesses below about 250 Å (i.e., in the regime where the layered 3D island growth occurs), but becomes more evident for the thicker films showing the cloudy topography.

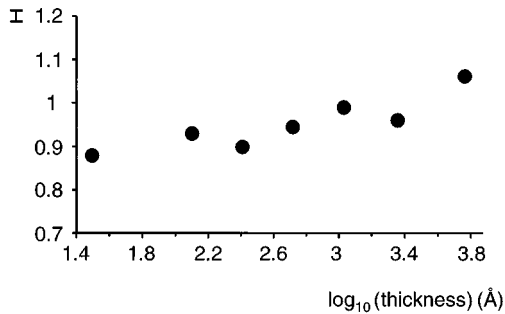


FIG. 3. The values of the roughness exponent H plotted as a function of the average Ag film thickness.

For all the plots shown in Fig. 2, the roughness increases with increasing length scale. For the flat Ag(111) substrate [Fig. 2(a)], no linear regime can be detected, indicating that the surface is not self-affine. After evaporation of Ag, a linear regime gradually develops [Figs. 2(b)–2(f)]. At the smallest length scales, deviations from the linear regime are observed. The tip shape and size impose a lower cutoff for the application of the scaling laws. Therefore, the roughness exponent H is determined via a least-square fit restricted to the data points belonging to the linear regime.

In order to emphasize the gradual increase of the roughness exponent H with increasing thickness, we have plotted the exponent H as a function of the total layer thickness t (see Fig. 3). For the smaller thicknesses ($t \leq 250$ Å), where 3D island growth occurs, the exponent varies between $H = 0.88 \pm 0.03$ (for $t = 31$ Å) and $H = 0.93 \pm 0.06$ (for $t = 123$ Å). For the thicker and more irregular films, the roughness exponent varies between $H = 0.95 \pm 0.03$ (for $t = 483$ Å) and $H = 1.06 \pm 0.03$ (for $t = 5001$ Å). At larger length scales, the error on the RMS roughness values is larger than the presumed 10%, since the roughness values could only be determined for a limited number of independent locations on the surface. Indeed, the atomically flat Ag(111) islands, on which the 3D islands grow, have a limited size of about 2000 Å. Consequently, the uncertainty on the roughness exponent H is larger than might be expected from the least-square fit to the data points and is estimated to be ± 0.1 . This implies that most values for H are close to 1 within the experimental error.

IV. DISCUSSION

In model calculations, the observed 3D island growth for film thicknesses below 500 Å has been predicted for epitaxial growth when there exists a barrier at the step edges that

prevents the atoms from diffusing across downward steps [18–21]. On top of the flat terraces, the incoming atoms can move to the upper step edges where they become incorporated in the Ag layer.

The scaling exponents have been estimated for several growth models. $H = 1$ has been found for a model describing molecular beam epitaxy (MBE) growth, where the relaxation process proceeds via surface diffusion [18,22]. This corresponds to the atomistic model where the atoms are allowed to relax via surface diffusion to positions with a maximum number of nearest neighbors [23].

Our results can also be interpreted in terms of a growth instability introduced by Villain [18], by Johnson *et al.* [24], and by Siegert and Plischke [25]. In their models, mounds are formed, which increase both in height and lateral size, until only one mound on the order of the system size remains [24]. As soon as the islands have reached this size, a rough surface starts to develop. In our experiment, the growth is clearly limited by the size of the underlying Ag(111) islands. A roughness exponent $H = 1$ (as in our case) was reported by Siegert and Plischke [25] for MBE growth where a growth instability is developing. In their model, the exponent H is only an effective exponent and does not describe the scaling anymore.

Experimentally, structures similar to ours have been observed for GaAs films grown by MBE methods on GaAs(100) substrates [24]. Furthermore, Ernst *et al.* [26] have observed unstable growth, resulting in a pyramidal-like surface profile, for Cu vapor deposited on a Cu(100) crystal at 160 and 200 K. In the latter case, exponents $H \approx 1$ were found, in agreement with our results.

V. CONCLUSION

We have studied the growth of Ag vapor deposited on Ag(111). For thicknesses below 250 Å, the growth proceeds via 3D island growth. For thicker layers, the surface becomes irregular. Roughness exponents H close to 1 have been obtained, in agreement with other experimental results as well as with theoretical models.

ACKNOWLEDGMENTS

Work at the K. U. Leuven was supported by the Belgian National Fund for Scientific Research (NFWO) and the Belgian Inter-University Attraction Poles (IUAP) and the Flemish Concerted Action (GOA) programs. Travel between Northeastern University and Leuven was supported through the NATO Collaborative Research Grant No. 931200. J. K. also acknowledges partial funding by the PRF Grant No. 27498-AC.

[1] P. Meakin, *Phys. Rep.* **235**, 189 (1993).
 [2] F. Family, *Physica A* **168**, 561 (1990).
 [3] *Fractal Growth Phenomena*, edited by T. Vicsek (World Scientific, Singapore, 1989).
 [4] *The Fractal Geometry of Nature*, edited by B. B. Mandelbrot (W. H. Freeman and Co., San Francisco, 1982).

[5] J. Krim and G. Palasantzas, *Int. J. Mod. Phys. B* **9**, 599 (1995).
 [6] H.-N. Yang, A. Chan, and G.-C. Wang, *J. Appl. Phys.* **74**, 101 (1993); H.-N. Yang and T.-M. Lu, *Phys. Rev. B* **51**, 2479 (1995).
 [7] I. Heyvaert, K. Temst, C. Van Haesendonck, and Y. Bruynseraede, *J. Vac. Sci. Technol. B* **14**, 1121 (1996).

- [8] F. Family and T. Vicsek, *J. Appl. Phys. A* **18**, L75 (1985).
- [9] F. Family, *Physica A* **168**, 561 (1990).
- [10] S. F. Edwards and D. R. Wilkinson, *Proc. R. Soc. London A* **381**, 17 (1982).
- [11] H. You, R. P. Chiarello, H. K. Kim, and K. G. Vandervoort, *Phys. Rev. Lett.* **70**, 2900 (1993).
- [12] G. Palasantzas and J. Krim, *Phys. Rev. Lett.* **73**, 3564 (1994).
- [13] A. Iwamoto, T. Yoshinobu, and H. Iwasaki, *Phys. Rev. Lett.* **72**, 4025 (1994).
- [14] C. Thompson, G. Palasantzas, Y. P. Feng, S. K. Sinha, and J. Krim, *Phys. Rev. B* **49**, 4902 (1994).
- [15] K. Fang, T.-M. Lu, and G.-C. Wang, *Phys. Rev. B* **49**, 8331 (1994).
- [16] S. Buchholz, H. Fuchs, and J. P. Rabe, *J. Vac. Sci. Technol. B* **9**, 857 (1991).
- [17] J. Krim, I. Heyvaert, C. Van Haesendonck, and Y. Bruynser-aede, *Phys. Rev. Lett.* **70**, 57 (1993).
- [18] J. Villain, *J. Phys. (France) I* **1**, 19 (1991).
- [19] G. Rosenfeld, R. Servaty, C. Teichert, B. Poelsema, and G. Comsa, *Phys. Rev. Lett.* **71**, 895 (1993).
- [20] J. Vrijmoeth, H. A. van der Vegt, J. A. Meyer, E. Vlieg, and R. J. Behm, *Phys. Rev. Lett.* **72**, 3843 (1994).
- [21] H. A. van der Vegt, H. M. van Pinxteren, M. Lohmeier, E. Vlieg, and J. M. C. Thornton, *Phys. Rev. Lett.* **68**, 3335 (1992).
- [22] Z.-W. Lai and S. Das Sarma, *Phys. Rev. Lett.* **66**, 2348 (1991).
- [23] D. E. Wolf and J. Villain, *Europhys. Lett.* **13**, 389 (1990).
- [24] M. D. Johnson, C. Orme, A. W. Hunt, D. Graff, J. Sudijono, L. M. Sander, and B. G. Orr, *Phys. Rev. Lett.* **72**, 116 (1994).
- [25] M. Siegert and M. Plischke, *Phys. Rev. Lett.* **73**, 1517 (1994).
- [26] H.-J. Ernst, F. Fabre, R. Folkerts, and J. Lapujoulade, *Phys. Rev. Lett.* **72**, 112 (1994).